The Surface Environment of the Small, Fast-Rotating Asteroid 2016 HO3. X. Li[1,2] and D. J. Scheeres[2], [1]School of Aerospace Engineering, Beijing Institute of Technology, 100081 Beijing, China, [2]Ann and H. J. Smead Aerospace Engineering Science Department, University of Colorado Boulder, Boulder, CO 80309, USA.

The study of small, fast-rotating asteroids will increase our understanding of the formation and evolution of rubble pile asteroids in general and extend our understanding of the surfaces of small asteroids. This abstract presents the results of our study of asteroid 2016 HO3 [1], recently officially named 469219 Kamo'oalewa. We consider the possible shape of this asteroid, its ambient environment and the possibility of regolith on its surface.

We find that asteroid 2016 HO3 is an elongate body with the ratio of its short and long axes being less than 0.4786. Due to its high spin rate (a period of 28.02 minutes), the surface of the asteroid has positive normal accelerations at low and mid latitudes. Despite this, it should be possible to retain millimeter to centimeter-sized grains on the surface as the required cohesion to do so is far smaller than that on the lunar surface (less than 0.2 Pa). The polar and short-axis regions should be able to keep some regolith and a zero-cohesive region exists at the asteroid poles (when modeled as an ellipsoid). Any regolith which detaches from the surface will escape from the asteroid, but grains starting their movement in different regions on the surface will exhibit different types of motions, including sliding, hopping and orbiting.

Our study provides important information that can be used to choose landing sites for surface, to perform scientific object assessment, or to develop trajectory designs for future exploration missions to 2016 HO3.

Shape of 2016 HO3:

First, the possible shape model of 2016 HO3 is established based on its measured light curves [2]. Due to limited observations, we build an ellipsoidal model of 2016 HO3 and focus on its three major axes denoted as a, b, c. Standard amplitude and magnitude methods are used to calculate the shape ratios [3,4]. Based on the known reduced brightness and magnitude of the light curve $H(\phi',0)=24.3$, $A(\phi',0)=0.8$ the aspect angle at the observation moment ϕ' and minimum brightness $H(90,0)$ are traversed to obtain the possible shape ratio of the ellipsoid. Figure 1 shows the possible sets of shape ratios. The results show that 2016 HO3 is likely an elongate body, which has a b/a ratio less than 0.4786. Based on a mean volumetric diameter of $d=36$ m, three specific shape models are built for the following study, I: $58.8\text{m}\times28.2\text{m}\times28.2\text{m}$, II: $66.04\text{m}\times31.60\text{m}\times22.36\text{m}$, III: $88.92\text{m}\times27.24\text{m}\times19.26\text{m}$. Meanwhile, the physical parameters of asteroid 2016 HO3 used in the study are listed in Table 1.

Table 1 Physical parameters of 2016 HO3

Density, kg/m^3	Spin Period	Diameter	Spectral Type
$\rho=2700$	$T=0.467$ h	$d=36$ m	L(S)

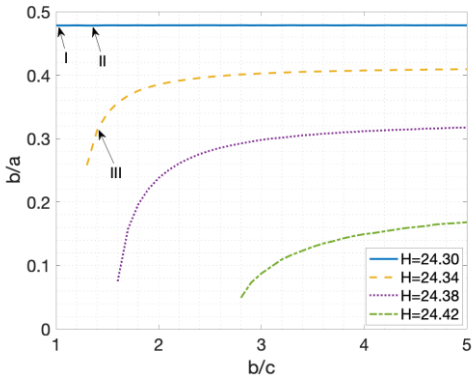

Fig. 1 Possible shape ratios with different $H(90,0)$

Surface Environment of 2016 HO3:

Based on these shapes and parameters, the gravity accelerations on 2016 HO3 are found to range between 1.10×10^{-5} m/s^2 to 1.33×10^{-5} m/s^2. Meanwhile, the high spin rate makes the low and middle latitude region have an outward normal acceleration. The zero normal acceleration boundary is between latitudes of 74.5 and 75.5 degrees and the poles, as shown in Fig. 2. Moreover, the sphere of influence (SOI) relative to the Sun is about 150 m on average, well beyond the surface of the body. The self-gravity force, solar radiation pressure and cohesive force on a particle are evaluated [5] and compared with the surface gravitational force. The results show that when analyzing the motion of micrometer to decimeter-sized particles, these ambient forces can be ignored except for the cohesive force.

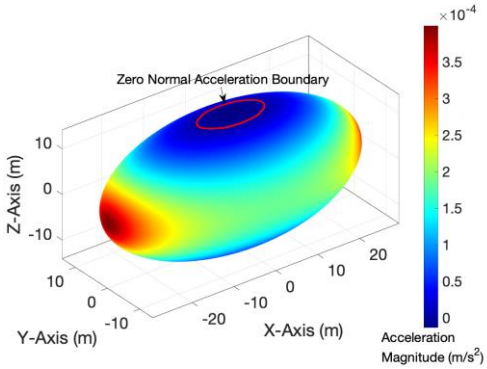

Fig. 2 Surface normal accelerations across the surface of the asteroid 2016 HO3

Analyzing the stability conditions for the cohesive regolith on the surface of asteroid 2016 HO3, we find two types of failure: landside and fission [6]. If the grain has a downward normal acceleration, the slope will fail when the tangential force acting on it exceeds the combined friction and cohesive force, or

$$\left\|\boldsymbol{a}_{gt}+\boldsymbol{a}_{rt}\right\| \geq \left|a_{gn}+a_{rn}\right| \tan\gamma + B\bar{g}, \quad a_{gn}+a_{rn}<0$$

Here $\boldsymbol{a}_{gt}, \boldsymbol{a}_{rt}, a_{gn}, a_{rn}$ are the tangential and normal component of the gravity acceleration and centrifugal acceleration on the surface, $\tan\gamma$ is the angle of fraction, B is the bond number, defined as the ratio between the cohesive force and the gravity on a particle and $\bar{g}$ is the mean gravity acceleration.

If the gravity is less than the rotation induced centrifugal force along the normal direction of the surface, the regolith will fail by fission, which happens when the total magnitude of the centrifugal force acting on the grain exceeds the combined force of gravity and cohesion, or

$$\left\|\boldsymbol{a}_{r}+\boldsymbol{a}_{g}\right\| \geq B\bar{g}, \quad a_{gn}+a_{rn}>0$$

Numerical analysis is made on the ellipsoidal models of 2016 HO3. With a friction angle $\gamma = 35^{\circ}$, the maximum bond number required to retain regolith is 29.4, and is at the end of the long axis. The value decreases when particles move from the long axis to the short axis and from the equator to the polar region. The critical bond number in the landslide failure region varies between 0 to 7.40. The zero-cohesive region exists in the polar areas with a surface radius of about 0.75 m. Based on the relation between particle size and cohesive force, the radius of particles for surface stability is approximately 0.1 m for the maximum bond number. Meanwhile, the required cohesion for surface stability in the fission region is 1.1×10^{-3} Pa for a millimeter particle and increases to 0.1 Pa for a decimeter particle. The required cohesion in the landslide region is much smaller.

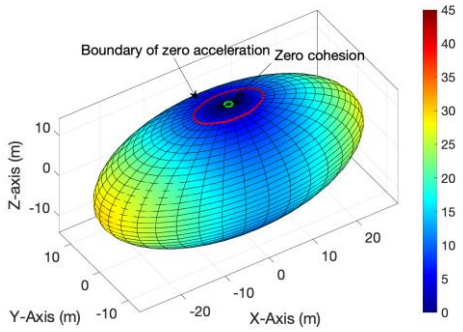

Fig. 3 Critical bond number of regolith on 2016 HO3

Further parameter analysis shows that increasing the density of the asteroid will increase the required cohesion to retain regolith of the same density, but enlarge the zero-cohesive region. The friction angle only affects the bond number in the landslide region. A larger friction angle will reduce the critical bond number and increase the size of the zero-cohesive region. Moreover, the maximum bond number increases if the asteroid has a smaller b/a ratio.

Dynamics of Regolith Wasting on Asteroid 2016HO3:

The motion of any surface regolith that is disturbed or has its connection to the surface broken can be analyzed using orbital dynamics and imperfect inelastic impact dynamics [7]. Due to its fast spin rate, it is found that all failed regolith will eventually escape from 2016 HO3. But particles in the landslide region and impact region for fission failure will undergo multiple periods of sliding and impacting before escaping.

The escape time and eccentricity of the escape trajectory are discussed and used to classify the region into several areas (Fig. 4). The motion of particles in each area are shown in Fig. 5. It is found that most particle re-impacts occur on the leading sides of the asteroid, and particles can transfer between the northern and southern hemispheres by hopping. Meanwhile, there are no re-impact points in the polar region, which means the regolith on poles is free from collisions due to regolith wasting. This analysis shows the polar region is the preferred landing site for surface exploration on asteroid 2016 HO3.

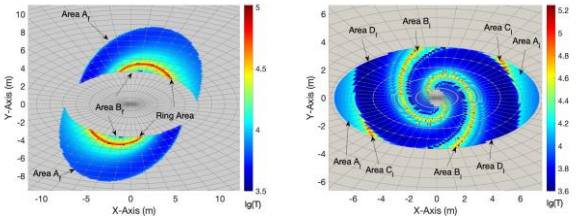

Fig. 4 Escape time in the impact and landslide regions

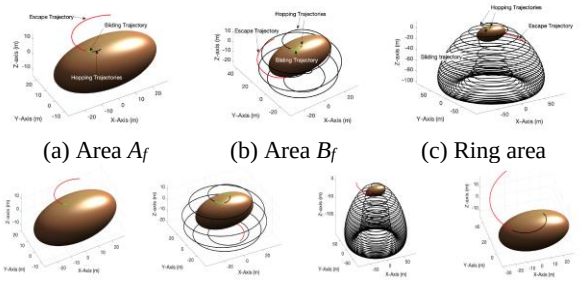

(a) Area A_f (b) Area B_f (c) Ring area

(d) Area A_l (e) Area B_l (f) Area C_l (g) Area D_l

Fig.5 Motion of failed regolith in different areas

References: [1] De la Fuente Marcos, C., and De la Fuente Marcos, R. (2016) *Mon. Not. Roy. Astron. Soc.*, 462, 3441–3456. [2] Reddy, V. et al. (2017). *AAS/DPS XLIX*, Abstract #49. [3] Magnusson, P. (1986) *Icarus*, 68, 1–39. [4] Michałowski, T. (1993) *Icarus*, 106, 563–572. [5] Scheeres, D. J. et al. (2010) *Icarus*, 210, 968–984. [6] Sánchez, P. and Scheeres, D. J. (2020) *Icarus*, 338, 113443. [7] Tardivel, S. et. al. (2014). J. Spacecr. Rockets, 51, 1857–1871.